Restorative Neurology and Neuroscience 31 (2013) 787–803
DOI 10.3233/RNN-139019
IOS Press

Local topographic influences on vision restoration hot spots after brain damage

Bernhard A. Sabel[a,*], Rudolf Kruse[b], Fred Wolf[c] and Tobias Guenther[a]
[a]*Institute of Medical Psychology, Computational Intelligence Research Group,Otto-von-Guericke-University of Magdeburg, Germany*
[b]*Department of Computer Science, Computational Intelligence Research Group,Otto-von-Guericke-University of Magdeburg, Germany*
[c]*Max Planck Institute for Dynamics and Self-Organization, Faculty of Physics, Georg-August University of Goettingen, Bernstein Center for Computational Neuroscience and Bernstein Focus Neurotechnology, Goettingen, Germany*

Abstract.
Purpose: Vision restoration training (VRT) in hemianopia patients leads to visual field enlargements, but the mechanisms of this vision restoration are not known. To investigate the role of residual vision in recovery, we studied topographic features of visual field charts and determined residual functions in local regions and their immediate surround.
Methods: We analyzed High Resolution Perimetry visual field charts of hemianopic stroke patients ($n = 23$) before and after 6 months of VRT and identified all local visual field regions with ("hot spots", $n = 688$) or without restoration ("cold spots", $n = 3426$). Topographic features of these spots at baseline where then related to (i) their respective local residual function, (ii) residual activity in their spatial neighbourhood, and (iii) their distance to the scotoma border estimated in cortical coordinates following magnification factor transformation.
Results: Visual field areas had a greater probability of becoming vision restoration hot spots if they had more residual activity in both local areas and in a spatially limited surround of 5° of visual angle. Hot spots were typically also located closer than 4 mm from the scotoma border in cortical coordinates. Thus, restoration depended on residual activity in both the local region and its immediate surround.
Conclusions: Our findings confirm the special role of residual structures in visual field restoration which is likely mediated by partially surviving neuronal elements. Because the immediate but not distant surround influenced outcome of individual spots, we propose that lateral interactions, known to play a role in perceptual learning and receptive field plasticity, also play a major role in vision restoration.

Keywords: Vision, plasticity, restoration, recovery, rehabilitation

1. Introduction

Plasticity of the visual system is not only involved in perceptual learning of the normal brain throughout life (Watanabe et al., 2002; Gilbert, 1994) but also provides the basis for spontaneous recovery of visual system damage (Sabel, 1999; Zhang et al., 2006). In patients with visual cortex injury, repetitive visual training (Sahraie et al., 2006; Bergsma and Van der Wildt, 2008., Gudlin et al., 2008; Kasten et al., 1998, 1999, 2000; Mueller et al., 2003, Polat, 2008; Sabel and Kasten, 2000; Sabel et al., 2004; Zihl and Cramon, 1985; for review see Sabel et al., 2011a) or non-invasive currents stimulation (Fedorov et al., 2011; Gall et al., 2010, 2011; Sabel et al., 2011b) can achieve vision restoration. The improved visual function is evident by increased performance in visual tasks and this has been explained by activation of residual visual structures (Sabel et al., 2011a, b). This is compatible with the observations that training-induced

*Corresponding author: Bernhard A. Sabel, Institute of Medical Psychology, Computational Intelligence Research Group,Otto-von-Guericke-University of Magdeburg, Germany. E-mail: bernhard.sabel@med.ovgu.de.

visual improvements after associated with electrophysiological changes (Julkunen et al., 2003) and functional imaging changes (Marshall et al., 2008; Pleger et al., 2003; Julkunen et al., 2006; Henriksson et al., 2007; Raemaekers et al., 2011).

While these findings inform us about the residual capacities and plasticity in visual recovery in general, little is known about possible neurobiological mechanisms underlying vision restoration on a local level. We believe that such mechanisms may include local influences of lateral interactions in visual cortex. Such lateral influences are known to be involved in perceptual learning (Gilbert, 1994; Gilbert et al., 2009) and receptive field plasticity (Calford et al., 2003; Gilbert and Wiesel, 1992), and it is likely that they might influence activities of surviving cells after incomplete lesions. In the present study we wished to explore the possible role of such lateral influences in vision restoration and therefore studied visual field chart dynamics of hemianopic patients that used vision restoration training (VRT), a repetitive perceptual learning task (training) aimed at strengthening the residual activity of surviving neuronal networks. Specifically, we reasoned that if receptive field plasticity is involved in vision restoration similar to that found in cats (Calford et al., 2000; Giannikopoulos and Eysel, 2006; Waleszczyk et al., 2003) or monkeys (Gilbert and Wiesel, 1992; Heinen and Skavenski, 1991), improvements should not be found at random locations in the visual field but should depend on specific topographic features indicative of receptive field plasticity.

Receptive field plasticity after retinal lesions is mediated by reorganisation of cortical connectivities through lateral interactions (Gilbert and Wiesel, 1992) and these are spatially limited by the extend of axonal arbors of cortical pyramidal cells. For example, receptive fields and visually driven spike activity can recover spontaneoulsy only 3.5–6 mm inside the lesion projection zone (Das and Gilbert, 1995; Giannikopoulos and Eysel, 2006; Heinen and Skavenski, 1991; Waleszczyk et al., 2003).

Such a spatial limitation of receptive field plasticity is also observed in the somatosensory cortex after digit amputation, where receptive field changes occur only within 500–700 μm around the initial cortical boundaries of the amputated digit representation (Buonomano and Merzenich, 1998). As computer simulations and physiological recordings from macaque area MT suggest, dynamic alterations in neural activation alone is sufficient to allow large receptive field changes after cortical damage (Sober et al., 1997). Cortical activity has been shown to be a critical factor for reorganisation in peri-lesion area of the primary sensorimotor cortex (Goodall et al., 1997) and in the retinal lesion projection zone in the primary visual cortex (Young et al., 2007). Thus, if reorganization of receptive fields is the underlying neuronal substrate of vision restoration, then it might be (i) mediated by areas which are not completely but only partially damaged, (ii) depend on peri-lesion and not long-distance, cortical activity, and (iii) visual field expansions should be spatially limited.

To study these hypotheses in hemianopic patients, we now charted in detail the topography of visual fields before vs. after training to first identify visual field spots which recovered ("hot spots") or remained unchanged ("cold spots"). By relating the location of those hot and cold spots to certain features of the baseline visual field topography, we wished to learn if the dynamics of visual field improvements is similar to rules of receptive field plasticity. As we now demonstrate, just as was observed in receptive field plasticity studies, vision restoration hot spots are not only dependent on local residual activity (defect depth) but they are associated with residual activity in a spatially limited surround.

2. Methods and materials

2.1. Study rational and hypotheses

Based on principles described above we expected that the following 3 topographic features would influence vision restoration: (i) the local detection probability of a stimulus at the spot itself, which is a function of whether the defect is absolute (sharp) or relative (diffuse), (ii) the aggregated detection probability in the local surround (perilesion area) and (iii) the distance to the scotoma border; the latter two features representing the concept of lateral interaction. Furthermore, to evaluate a possible role of eye movements we extracted variables that consider possible eye movement artifacts.

2.2. Subject sample

The visual field of hemianopic subjects ($n = 23$, 16 male, 7 female) was assessed before and after carrying out a 6 months stimulation training (vision restoration

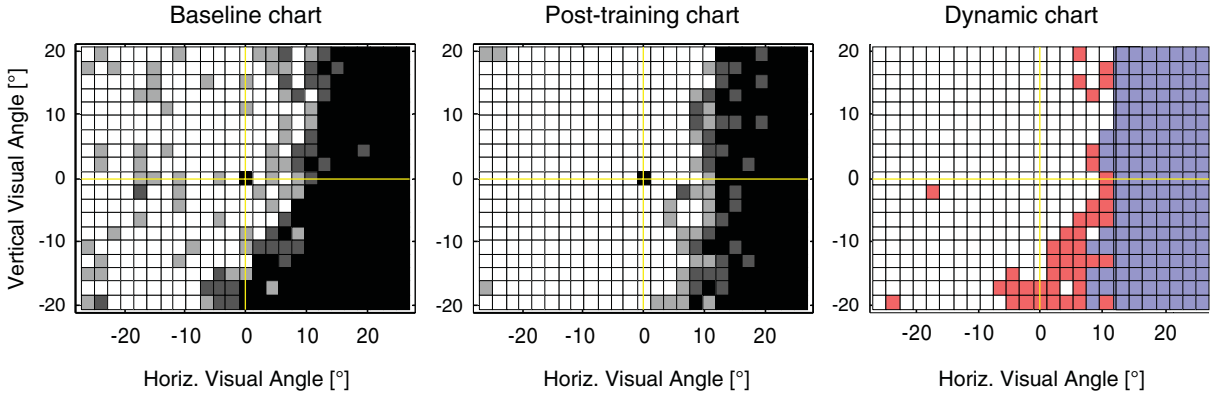

Fig. 1. Baseline chart (left panel) and post-training chart (middle panel) after 6 months of stimulation training from subject No. 8. Intact areas are shown as white, areas of absolute-defect (blind) in black and residual areas with mild- or moderate-defect in different shades of grey. The right panel displays the "dynamics chart" which was calculated by comparison of post-training with the baseline chart. The false-colour displays the occurrence or lack of restoration. Hot spots (red) are positions with restoration; spots without restoration (cold spots) are shown in blue and healthy positions at baseline (they were excluded from the analysis) are shown in white. The charts of all 23 subjects are available in the additional materials section.

therapy, VRT). The data were retrospectively selected from a pool of subjects which have previously been trained in Magdeburg in the course of two independent studies (Mueller et al., 2003).

These experiments were undertaken with the understanding and written consent of each subject according to the Code of Ethics of the World Medical Association (Declaration of Helsinki of 18 July 1964) and they were approved by the local ethics committee of the University of Magdeburg.

The subjects were 52 ± 13 (mean $\pm$ SD) years old at start of training and their visual field defects were caused by post-chiasmatic damage of the visual system (age of lesion: 1.2 ± 1.3 yrs in study 1 and 3.8 ± 1.1 yrs in study 2). To be included in the present study the following inclusion criteria had to be met: stroke or ischemia in the occipital cortex (A. cerebri posterior or A. media) as evidenced by medical documentation, and the availability of at least 3 independent visual field diagnostic tests at baseline and post-training, respectively. These three visual field tests were then superimposed to generate visual field charts as shown in Fig. 1. Exclusion criteria were (i) confounding eye disease, such as nystagmus or strabismus, (ii) more than 4 % false positive positions at baseline or post-training examination in HRP, and (iii) less then 90% of detected fixation catch trials in HRP.

On the basis of the visual field charts at baseline, the visual field defects (22 homonymous, 1 heteronymous) were classified as follows: hemianopia to the left ($n = 10$) or to the right side ($n = 4$), quadrantanopia in the upper ($n = 2$) or lower left quadrant ($n = 1$), quadrantanopia in the upper right quadrant ($n = 2$), quadrantanopia with partial defect in multiple quadrants ($n = 3$) and local scotoma ($n = 1$).

2.3. Charting the visual field

Before and after 6 months of VRT, high-resolution perimetry (HRP) charts were obtained as previously described (Kasten et al., 1997). The visual field was measured by presenting static above-threshold visual stimuli in random sequence on a monitor controlled by a computer. The stimuli were positioned in a predetermined rectangular grid-like fashion at high spatial resolution of 474 test positions within a 55° visual angle. Three such HRP charts were tested in separate sessions and subsequently superimposed to be able to locate areas of residual vision, as displayed in Fig. 1. The distance of the eyes from the monitor was 30 cm (visual field angle: 55°, study 1) or 40 cm (visual field angle: 42°, study 2). For subsequent analysis we modified the charts to account for this difference in monitor distance. We used above-threshold target stimuli (size: 0.57° in study 1 and 0.43° in study 2) with a bright grey appearance (luminance: 86 cd/m² in study 1 and 48 cd/m² in study 2) on a dark background (luminance: 23 cd/m² in study 1 and 0.2 cd/m² in study 2). These target stimuli were presented for 150 ms at random positions in a 25×19 grid. The inter-stimulus interval varied randomly between 1000–2000 ms. A "hit" was a correct response to the

target presentation and it was only counted if the subject responded to the stimulus presentation within a valid time-window of less than 1000 ms by pressing a key on the keyboard of the computer. Responses before and after the valid time window are termed "false positives". These false positives are comprised of either random reactions unrelated to the stimulus presentations or reactions which are delayed, i.e., which are >1000 ms. Each diagnostic HRP session lasted 20–25 minutes. All subjects were tested binocularly while the head was stabilized by a chinrest to reduce the influence of head and body movements. The objectivity, validity and retest reliability of this diagnostic test have been described elsewhere (Kasten et al., 1997). Although the parameter sets differ between both studies from which the subjects were taken, we found no significant differences (two-tailored *T*-test) in the response times in the baseline ($\mu_1 = 450 \pm 16.5$ ms, $\mu_2 = 448 \pm 12.8$ ms) or in the post-training diagnostic charts ($\mu_1 = 427 \pm 11.0$ ms, $\mu_2 = 415 \pm 10.0$ ms).

VRT was applied as previously described (Kasten et al., 1998). Firstly, blind regions of residual vision were identified in the HRP charts as shown in Fig. 1. Secondly, training regions were selected to primarily include areas of residual vision which are typically located at the visual field border (the definition of areas of residual vision is given below). For charts which contained none or only few areas of residual vision, the training region was defined to include areas of similar size to both sides of the border. Visual stimuli were then presented in these training regions and the subjects had to respond to each training stimulus by pressing a key on the keyboard in a manner similar to the diagnostic session. Training lasted on average for about 1 hr. daily and the training area was adjusted monthly or more frequently as necessary, depending on the subject's progress.

2.4. Topographic maps: Definition of terms

There are three different charts on which the subsequent analysis was based: (i) "baseline charts" of the visual field as documented by HRP, (ii) "post-training charts" after VRT and (iii) "dynamic charts", which are created by calculating the difference between the respective baseline and post-training chart.

The term "blind region" denotes the sub-sector of the visual field with an absolute defect; it is identical with the established term "scotoma" or "hemianopic field". "Intact regions" are those unaffected by the injury with perfect or near-perfect detection performance. The term "areas of residual vision" (ARV) corresponds to the well known term "relative defect" and is characterised by impaired, but not absent, vision. Here, the response time is slower (Sabel and Kasten, 2000) and the probability of being able to detect super-threshold stimuli is reduced (Kasten et al., 1999).

The HRP visual field consists of 474 spots which are the smallest units of the measured visual field. Each of the 474 spots on the HRP baseline-chart was classified as to their detection probability (residual function), i.e., how often the subject detected the target stimuli given the specific background and stimulus luminance parameters employed in our study. Thus, each spot indicates a specific functionality state. "Intact function" is shown in white (subject responds correctly to 3 out of 3 stimulus presentations), "mild-defect" is shown in light grey (subject responds to 2 stimulus presentations), "moderate-defect" is shown in dark grey (subject responds to 1 stimulus presentation) and "absolute-defect" is shown in black (subject does not respond to any of the stimulus presentations in this area). For the purpose of further analysis we pooled the moderate-defect spots and absolute-defect spots to one class termed "impaired spots". Likewise, the term "healthy spots" represents the categories mild-defect and intact spots.

2.5. Dynamic charts

Dynamic charts visualise the change over baseline after 6 months VRT for each patient. Just as in the baseline chart, the dynamic chart is subdivided into identical squares. Each square was assigned a false colour after calculating the difference between the baseline and the post-training HRP chart for each subject. Depending on their respective "change over baseline", dynamic spots are defined as follows: (i) spots which were impaired spots at baseline and became "healthy" spots were termed "hot spots", and (ii) spots which were impaired spots at baseline and were still impaired post-training were termed "cold spots". These detection differences were calculated for each visual field spot, and these were then combined to created "dynamic charts" (see Fig. 1, right panel).

2.6. Measuring fixation

Some authors have suspected that visual field expansions as measured in HRP may be mediated solely by

eye movements during diagnostic sessions. To assess the influence of eye movements, we therefore measured fixation performance during diagnostic sessions using a fixation task. Here, reactions to an isoluminant colour change (random in time) of the fixation spot (luminance: 100 cd/m² in study 1 and 28 cd/m² in study 2) located at the centre of the presentation screen were recorded (on average after 4 target stimulus presentations).

The isoluminant alternation of the coloured fixation spot can be detected with 100% confidence only with foveal vision. Experiments with healthy subjects ($n = 17$) showed that the detection ratio of isoluminant colour changes as used as fixation control drops below 90% when the stimuli are presented beyond 2° eccentricity (unpublished observations). In that study we also confirmed that the number of acknowledged fixation catch trials is associated with the number of eye movements which were made during the diagnostic test: the more eye movements a subject made, the fewer fixation catch trials were acknowledged by the subject.

Hence, while we cannot completely exclude the possibility that eye movements may have had some influence during the diagnostic sessions, by using fixation catch trials as criteria we accounted for eye movements during the diagnostic session indirectly, and could thus exclude diagnostic sessions with insufficient fixation, thus reducing the impact of eye movements. Accordingly, a visual field chart was included in our analysis only if 90% or more of the approximately 100 fixation control presentations were detected in HRP. For this we superimposed 3 repeated tests, i.e. a total of 300 fixation catch trials which were presented at random intervals. Additionally, the experimenters observed the subjects' eyes during the entire diagnostic session to ascertain proper fixation and alertness of the subject.

2.7. *Influence of topographic features on restoration of vision*

Our study focuses on the influences of topographic features on the observed restoration. We examined features based on the local topography and considered the number of detected fixation catch trials in order to identify the effect of eye movements on the occurrence of hot spots.

The following features are comparable to those which were either studied in physiological plasticity experiments or those guided by our experience. Note, however, that these specific features constitute only a small fraction of all possible features. We were particularly interested in measuring local influences on restoration and therefore analyzed how the topographic position of cold and hot spots are related to (i) the detection probability of test stimuli at baseline (*Residual-Function*), (ii) the aggregated detection probability of test stimuli in their surround (radius: 5°, *Neighbourhood-Residual-Function*) and (iii) their cortical distance to the scotoma border (*Distance-to-Scotoma-Border*). The cortical distance is measured at baseline in cortical millimeters by using a retinotopic model. The features, their respective range of values and graphic representations are summarised in Fig. 2.

2.7.1. *Feature 1: Residual-Function*

With the "*Residual Function*" feature we wished to observe whether or not the functional state of a given visual field spot in the baseline diagnostic chart is associated with the restoration potential of the very same spot. *Residual-Function* is expressed as the detection probability of test stimuli, (shown in false colour of black, white and different shades of grey, see Fig. 1 left). Note that *Residual-Function* is not a measure of individual electrophysiological activity of single neurons but it is the overall residual function of the corresponding region probed by the stimulus detection. It shows how often the subject has responded to a total of 3 stimulus presentations (detection rate) per specific test position (see above). Grey spots are of special interest as they represent areas of residual visual functions. The value assignments were as follows (see Fig. 1): intact area = 1 (white), mild defect = 0.66 (light grey), moderate defect = 0.33 (dark grey) and absolute defect = 0 (black). Using these values we determined whether moderate-defect spots have a greater potential of becoming hot spots than spots that lack any residual vision (spots with an absolute-defect).

2.7.2. *Feature 2: Residual-Function of spatial neighbourhood*

We also wished to learn if and how the *Residual-Function* (measured at baseline) in the immediate surround of hot and cold spots – called the "spatial neighbourhood" – is associated with the restoration at single spots. The spatial neighbourhood around a hot or cold spot included all tested spots in areas within a 5° radius of visual angle. This limit to 5° in visual space (see Fig. 3) was chosen for technical reasons: firstly, larger values would possibly average out local

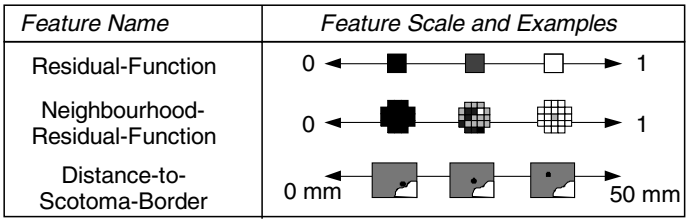

Fig. 2. Feature units, showing examples of the scale ranges (minimal and maximal).

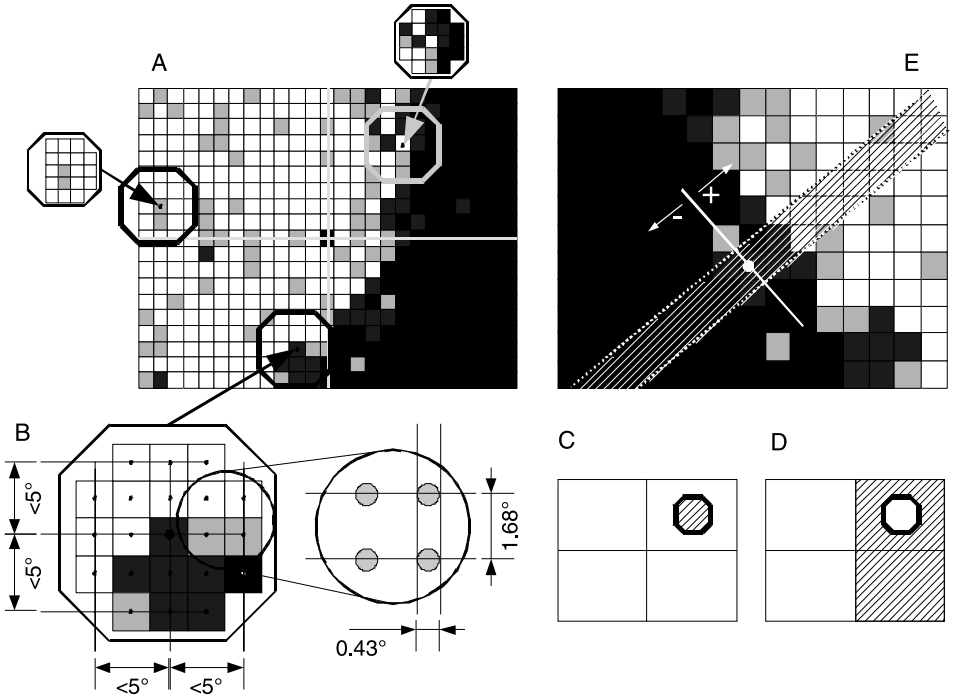

Fig. 3. Part A: This graph illustrates the extraction of three spatial neighbourhoods from the baseline diagnostic chart. Part B: The spatial neighbourhood has a radius of 5° in visual field coordinates. Stimulus size is 0.43°, interstimulus space is of size 1.68° (values of study 2). Part C: The Neighbourhood-Residual-Function is computed on the basis of the spot's spatial neighbourhood (hatched area). Part D: The Hemifield-Residual-Function is computed on the basis of the spot's hemifield minus the spot's spatial neighbourhood (area with hatching). Part E: The spatial neighbourhood was examined one-dimensionally but with high spatial resolution in a thin corridor (area with hatching between the 2 dashed lines) which is defined by any selected spot (white circle) and runs orthogonal to the scotoma border. Positive distances are assigned to the part of the corridor in direction to the intact area and negative distances are assigned to the part of the corridor in opposite direction to the intact area.

effects and, secondly, much smaller values are below the spatial resolution of the diagnostic test grid.

The *Neighbourhood-Residual-Function* is a measure of how much residual function is present in the entire neighbourhood. This parameter is calculated by taking the average *Residual-Function* (at baseline) of all stimulus positions in the entire 5° radius (see Fig. 3C), i.e., the functional state of the entire neighbourhood. Therefore, a value of "1" is assigned to a neighbourhood where all spots are intact and "0" if all spots in the neighbourhood are absolute-defect. The calculation does not include the *Residual-Function* of the spot in the neighbourhood centre (the *Residual-Function* of the centre spot was addressed above) nor does the calculation include spots of the contralateral hemifield. We were interested in whether spots surrounded by many intact areas have a higher chance of restoration than spots surrounded by many defective

areas; we expected that greater functionality in the surroundings at baseline would increase the chance of restoration in the centre.

In order to test whether any difference in the *Residual-Function* between hot and cold spot exists only locally or in the complete hemifield, we also tested the *Residual-Function* of all stimulus positions in the ipsilateral hemi-field (where the testing spot is located) while excluding the directly adjacent spatial neighbourhood of 5° (see Fig. 3D).

We have also analyzed *Neighbourhood-Residual-Function* as a function of cortical distance (measured in cortical millimeters). This analysis was restricted (i) to moderate-defect spots, (ii) to the orthogonal orientation of the scotoma border and (iii) to the ipsilateral hemifield. Only moderate-defect spots are considered because the moderate-defect spots are typically located around the scotoma border and are almost equally distributed among cold and hot spots (45% of moderate-defect spots are cold spots and 55% are hot spots). This contrasts with absolute-defect spots which usually form huge homogeneous areas of cold spots. The second restriction is necessary to reduce the artefact which results from the high distances to the spots from the often coast-like form of the scotoma border. Therefore, the examined neighbourhood

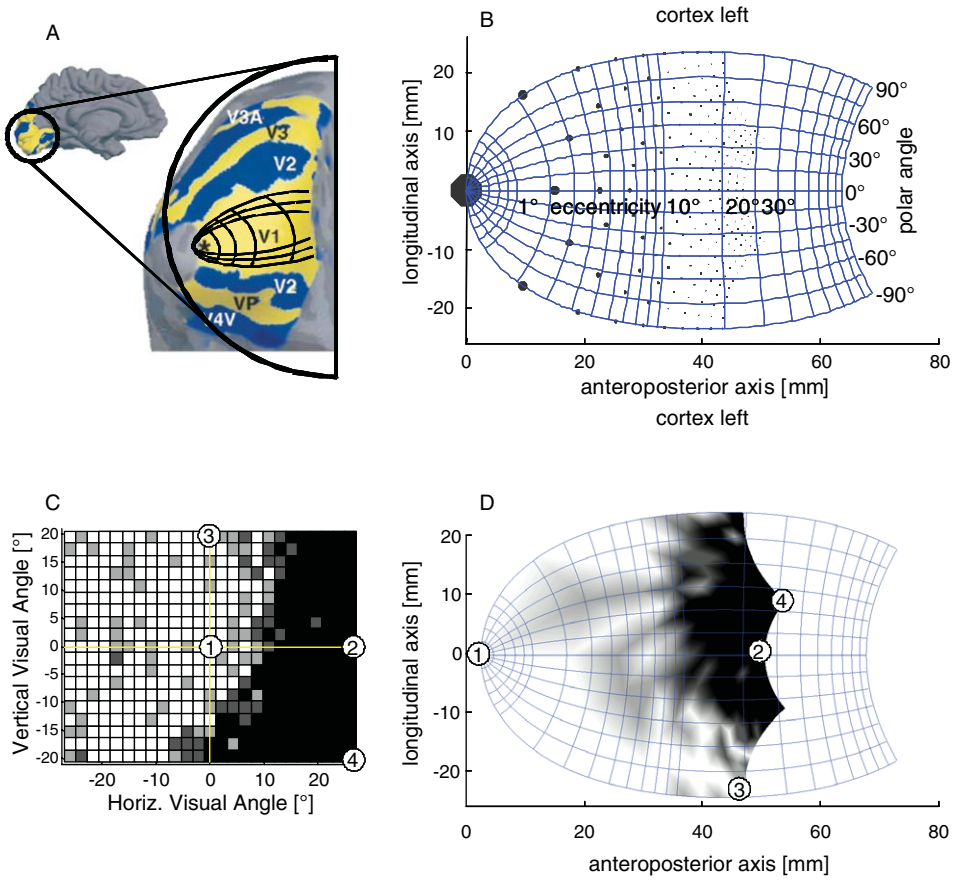

Fig. 4. Part A: Sagittal view of the left cortex. The primary visual cortex (circle in inset) is inflated and borders between the different visual areas (V1–V4) are shown (figure adapted with kind permission from (Tootell et al., 1998)). Iso-polar coordinate lines of the projection model are superimposed. They originate from the foveal confluent (marked with a star). Part B: Positions of HRP stimuli as used in baseline assessments projected onto the primary visual cortex following transformation of the visual field coordinates according to the cortical magnification factor. Part C: The visual field map of subject 8. Four landmarks are shown (1 fixation point at fovea, 2 the maximum horizontal distance of the hemianopic field to the outer limit of the test, 3 the maximum vertical distance to the lower testing limit, 4 the position with greatest eccentricity). Part D: The right hemianopic field of subject 8 is projected here onto the left cortical hemisphere in V1. To follow the results of the coordinate transformation, landmarks defined in C were drawn at their corresponding cortical positions. Although the damage in the right hemifield is broad, the scotoma is much smaller in cortical coordinates due to cortical magnification.

is only one dimensional and considers spots which are located on a virtual line connecting the spot and the border position of minimal distance to the spot; hence the orientation is orthogonal to the border (see Fig. 3E). Thirdly, the analysis is restricted to the ipsilateral hemifield because the contralateral hemisphere (which is typically intact) would otherwise interfere with our analysis. This analysis of *Neighbourhood-Residual-Function* as a function of cortical distance requires the transformation of diagnostic maps into cortical maps (see below).

2.7.3. *Cortical magnification and visual cortex charts*

We transformed the visual field data obtained in HRP (a campimetric measure) into cortical coordinates to reduce possible artefacts in vision restoration caused by the cortical magnification factor. Cortical magnification is relevant because stimuli presented in HRP are always of the same size and brightness and of equal distance to each other in the visual field chart, regardless of their respective distance from fixation (eccentricity).

To accomplish this transformation of visual field charts to visual cortex charts we used the function of cortical magnification which are known for the visual cortex (Dougherty et al., 2003). Results from retinotopy studies (Schwartz, 1977) suggest that the complex logarithm describes the transformation from visual space coordinates to visual cortex coordinates. A model which adequately represents primate visual cortex topography is modeled after the visual cortex of the owl monkey (Balasubramanian et al., 2002). While this model incorporates the V1, V2 and V3 cortical areas, we only considered the V1-part of the model. The model describes the function of eccentricity and polar angle in relative cortical coordinates. Absolute scales were obtained by adjusting the model to the observed average human V1 surface area of 2383 mm² (Andrews et al., 1997). We applied this retinotopic model on visual space coordinates and thus obtained visual cortex coordinates for the visual field charts of each of our subjects (see Fig. 4); however, we were aware of the great inter- and intra-individual variances in the cortex sizes which may vary by a factor of up to 2.5 between subjects (Andrews et al., 1997; Dougherty et al., 2003). Since imaging data were not available for all patients we reasoned that the variance introduced by this uncontrolled factor would – if anything – introduce a bias against our hypothesis and would therefore be permissible.

In HRP, adjacent visual field chart positions are equidistant (1.68°) to each other in visual space coordinates (see Fig. 3). Following the transformation to cortical coordinates, the minimal distance of adjacent baseline stimulus positions in visual cortex coordinates is 0.63 mm for peripheral eccentricity positions and as large as 15 mm in the fovea.

2.7.4. *Feature 3: Distance-to-scotoma-border*

With this feature we wished to study if the distance (measured in cortical coordinates) of a given spot to the scotoma border (at baseline) influences the probability of restoration, i.e., the likelihood that a hot spot is observed. The scotoma border was defined as the border between defect and the intact or residual area by a 4-step algorithm. (i) A median filter was used to reduce noise in the diagnostic maps (which may be caused by attentional deficits during the visual field testing). (ii)

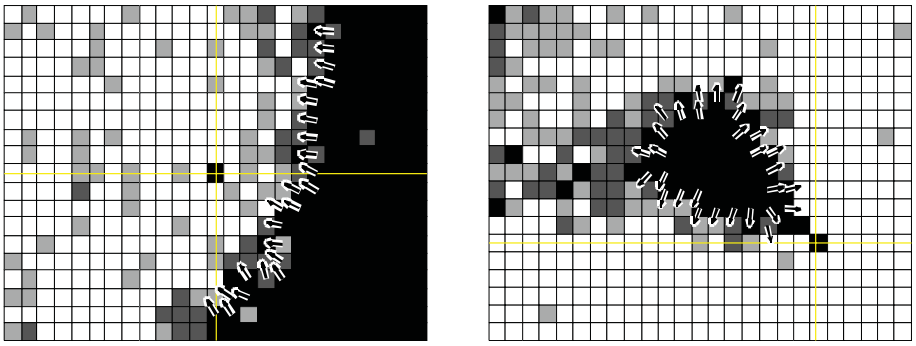

Fig. 5. Distance between hot spot and the intact-defect border. After the visual field border was automatically detected (shown by arrows) the cortical distance was computed between hot spots, cold spots and the border. Left: This border area has the form of a "coast" running almost vertically in parallel to the zero vertical meridian. Right: The border is ring-shaped; the scotoma is surrounded by intact areas in most directions. The information about the orientation of the border is used for orientation of the corridor in Fig. 3E.

The orthogonal border orientation and border position was measured by convolution with horizontal and vertical gradient kernels (the border orientation is used for orienting the corridor, see Fig. 3E). (iii) The vector field thus obtained (each vector has a horizontal and a vertical component) was smoothed by a Gaussian kernel (size 3×3). (iv) Vectors in absolute-defect areas which do not border residual or intact areas were deleted. The result was an automatically detected border with orthogonally oriented border vectors pointing towards the intact area (see Fig. 5). The Euclidean distance was measured in cortical coordinates between the spot and its next proximal border position. The analysis was restricted to one hemifield only. Possible inter-hemispheric interactions in the visual system were not considered in our analysis.

2.7.5. *Correlation of features and training outcome*

Two correlation coefficients were calculated to quantify the statistical relationship between the topographic features and training outcome. The first correlation (Pearson's Rho) was subject-based and establishes the relationship between topographic features and the number of observed hot spots per subject. This correlation required the replacement of the original features by dummy variables because the topographic features are spot-related whereas the number of observed hot spots per subject is chart-related (and therefore subject-related). Each feature variable was divided into two intervals (the lower and the upper interval) by using the median of the data distribution of the respective feature (we used the complete set of spots collapsed among all subjects). A subject related dummy variable was obtained by counting the number of spots in each subject chart contained in the upper interval (in the case of *Residual-Function and Neighbourhood-Residual-Function*) or contained in the lower interval (in the case of *Distance-to-Scotoma*). The second correlation was based on the spots value, exclusively. In order to examine whether with respect to the specific topographic features at baseline a location with high or low values showed post-training restoration or not, we correlated (ranking based non-parametric Spearman's Rho) each spot's feature value with its dichotomous post-training classification (cold or hot spot). In order to perform this correlation independent of subjects we used the following modified bootstrap resampling method: (i) prepare 23 sets $\prod_1$ to $\prod_{23}$ such that $\prod_i$ contains all spots of the i-th subject (a spot itself was represented by its value of the respective feature and its post-training classification); all $\prod_i$ together form the set $\sum = \{\prod_1, \ldots, \prod_{23}\}$. (ii) Draw only one sample π_i from each $\prod_i$ with replacement resulting in a sample set of spots $\sum^* = \{\pi_1, \ldots \pi_{23}\}$. (iii) Compute the Spearman correlation coefficient ρ on the basis of each spot's feature value and its dichotomous training outcome (cold or hot spot) of $\sum^*$. (iv) Repeat the second and third step for 1000 iterations resulting in the correlation coefficients ρ_1 to ρ_{1000}. (v) Compute the median among all ρ_i. As the result of these steps, a subject-independent correlation measure was obtained for the spot's restoration response (hot or cold). On the basis of the distribution of the ρ_i, 95% confidence intervals were computed to test for statistical significance.

2.7.6. *Fixation-performance*

The fixation performance at baseline and at post-training charts was correlated with the number of hot spots per subject. Hence, if eye movements are related to the occurrence of hot spots in the subject sample, a negative correlation between acknowledged fixation catch trails and number of hot spots would be expected. However, the validity of this analysis is limited because we included only subjects in our study with excellent (>90%) fixation performance.

3. Results

In order to compare the extent of restoration of our patient sample with patient samples from other studies we calculated their detection gains. On average, our subject sample improved from 293.6 ± 12.4 detected

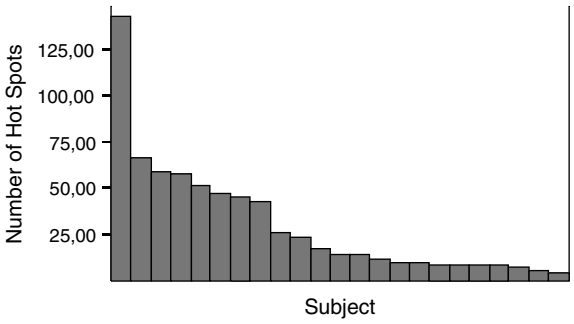

Fig. 6. Number of hot spots after vision restoration training for each of the 23 subjects.

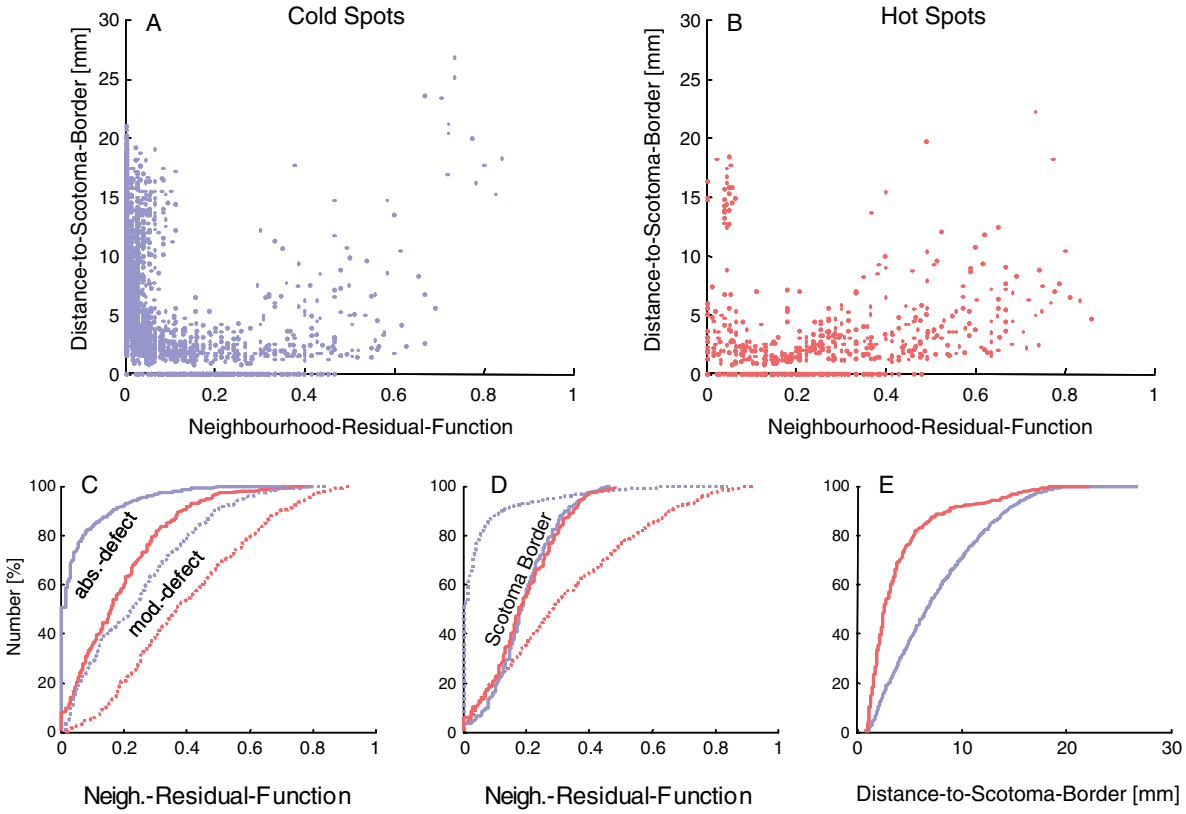

Fig. 7. The scatter plots of cold (A, blue) and hot (B, red) spots with respect to Neigh.-Residual-Function and Distance-to-Scotoma-Border. The spots of all subjects are collapsed into one graph. C: The cumulative distribution of Neigh.-Residual-Function is shown separately for moderate-defect (dashed) and absolute-defect (solid) spots. D: The cumulative distribution of Neigh.-Residual-Function is shown separately for spots located on the Scotoma Border (solid, Distance-to-Scotoma-Border = 0) vs. beyond the Scotoma Border (dashed, Distance-to-Scotoma-Border > 0). E: The cumulative distribution for Distance-to-Scotoma-Border in cortical coordinates (spots with Distance-to-Scotoma = 0 are not considered in the graph).

stimuli before to 322.5 ± 12.7 after training (of a total of 474 test stimuli). The average absolute improvement was thus $6.0 \pm 2.7\%$ (mean $\pm$ S.E.; $p = 0.01$, paired T-test) which is in the range of prior studies (Kasten et al., 1998; Mueller et al., 2003; Poggel et al., 2004; Sabel et al., 2004).

Considering that 23 subjects were studied with 474 testing positions each, across all subjects we collected a total sample of 10.902 baseline visual field spots of which 688 spots were "hot spots" and 3.426 were "cold spots". Figure 6 shows the distribution of hot spots among all subjects.

The distribution of hot and cold spots with respect to *Distance-to-Scotoma-Border* and *Neighbourhood-Residual-Function* is shown in Fig. 7a and b.

We calculated the mean value of all features for hot (μ_{hot}) and cold spots (μ_{cold}) separately and reduced the influence of the individual subject's performance on the averages for cold and hot spots by first calculating the average for each subject regarding the two groups of hot and cold spots and then calculating the average among all subjects for the respective group of hot and cold spots (2-tailed Mann-Whitney-U-Test).

3.1. Residual-Function

Hot spots ($\mu_{hot} = 0.16 \pm 0.01$) have a significantly higher Residual-Function at baseline than cold spots ($\mu_{cold} = 0.04 \pm 0.01$) ($p < 0.01$). At baseline, hot spots consist of absolute-defect and moderate-defect spots in similar proportion (46% were moderate-defect, 54% were absolute-defect). Contrasting this, 93% of cold spots were absolute-defect at baseline and only 7% were moderate-defect. Thus, a spot with a detection

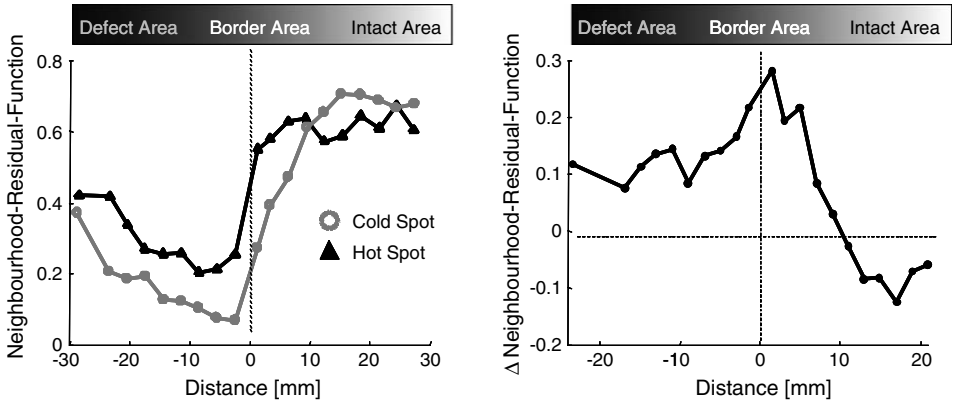

Fig. 8. Left panel: Neighbourhood-Residual-Function of cold and hot spots (collapsed into one set from all subjects) as a function of distance measured from hot and cold spots. Only moderate-defect spots which are typically found near the intact defect border are considered. The examined spatial neighbourhood is one dimensional and restricted to a thin corridor located on a virtual line which runs orthogonal to the scotoma border (see Fig. 3E). The corridor itself is limited to the damaged hemifield. Positive distances are assigned to the part of the corridor oriented toward the direction of the intact area and negative distances represent the opposite direction. Right panel: The difference of both functions (hot minus cold) shows that the maximal difference, which is equal to more than 1/5 of the complete scale, is found <4 mm from the neighbourhood centre.

probability of 33% (moderate-defect) at baseline will likely become a hot spot.

3.2. *Neighbourhood-Residual-Function*

The feature *Neighbourhood-Residual-Function* measures the average probability of stimulus detection (at baseline) in the local spatial neighbourhood of a 5° radius around cold and hot spots. We found that hot spots have a significantly ($p < 0.01$) higher *Neighbourhood-Residual-Function* ($\mu_{hot} = 0.37 \pm 0.03$) than cold spots ($\mu_{cold} = 0.10 \pm 0.03$) in their respective spatial neighbourhoods. This demonstrates that hot spots are surrounded by significantly more intact areas or areas of residual vision than cold spots.

When the residual function of the complete hemi field was computed (excluding the 5° surround) we found that the *Hemifield-Residual-Function* was not statistically different between cold ($\mu_{cold} = 0.32 \pm 0.05$) and hot spots ($\mu_{hot} = 0.34 \pm 0.05$). Thus, the complete hemifield did not contain more intact areas around hot spots than around cold spots. From this we conclude that the influence of residual function on restoration is limited to the immediate neighbourhood.

In order to examine the influence of residual vision in the immediate surround of cold and hot spots in finer spatial resolution, we measured *Neighbourhood-Residual-Function* as a function of continuous cortical distance. Similar to the results presented above, we found a higher residual function around hot spots in comparison to cold spots in the immediate neighbourhood of the cold or hot spot (see Fig. 8). The maximal difference (>1/5 of the complete scale) was observed within a distance of 4 mm respectively in the direction of the intact and the defective area.

To study how the *Residual-Function and Neighbourhood-Residual-Function* factors interact, we have plotted the number of cold and hot spots in a cumulative function (Fig. 7C). Generally, the neighbourhood was found to be more active around moderate-defect spots than around absolute-defect spots (independent of the classification of cold or hot spots).

Another interdependent relation of *Neighbourhood-Residual-Function* was found with the feature *Distance-to-Scotoma-Border*. As Fig. 7D shows, the neighbourhood does not differ between hot and cold spots as long as they are located near the scotoma border. In contrast, if hot and cold spots are located at some distance from the scotoma border, the neighbourhood around hot spots was found to be significantly more active than around cold spots.

3.3. *Distance-to-Scotoma-Border*

We further wished to learn how restoration is associated with the distance of the hot spots from the scotoma border. In order to consider cortical mag-

Table 1
Correlation coefficients between features and training outcome in a resampling design at the level of the spots (second column, Spearman's Rho) and at the level of individual subject charts (third column, Pearson's Rho). The number of spots per subject which satisfy (i) Residual-Function identical to 0, (ii) Neighbourhood-Residual-Function above the median of 0.03 and (iii) Distance-to-Scotoma-Border below the median of 4.93mm was measured

Feature	Spearman correlation with type of spot (cold, hot)	Pearson correlation with number of hot spots per subject
Residual-Function	0.73**	0.70**
Neighbourhood-Residual-Function	0.59**	0.56**
Distance-to-Scotoma-Border	−0.19	0.44*
Baseline fixation	N.A.[1]	0.17
Post-training fixation	N.A.[1]	0.07

Abbreviations: **=correlation significant at the 0.01 level, *correlation significant at the 0.05 level. 1: Note that a correlation with individual spots is not possible.

nification, this analysis was carried out using visual cortex coordinates. Hot spots ($\mu_{hot} = 3.2 \pm 0.67$ mm) were typically found closer ($p < 0.01$) to the scotoma border than cold spots ($\mu_{cold} = 5.9 \pm 0.65$ mm). As Fig. 7E shows, the majority of hot spots (75%) were located within 4 mm from the scotoma border.

3.4. Correlation of topographic features with training outcome

To quantify the statistical relationship between the topographic features and the training outcomes, two correlation coefficients were calculated. (i) We measured the correlation (Pearson's Rho) between the topographic features and the number of observed hot spots per subject, hence, only the number of occurrences in a chart was considered, independent of their respective location. (ii) To measure the spot, and location-based correlation, the topographic features were computed for all spots together and then correlated (Spearman's Rho) with their training result (hot or cold). In order to perform the latter correlation independent of subjects, we used a specific resampling method (see methods section).

We found significant correlations between the training and the topographic features (*Distance-to-Scotoma-Border* correlates significantly only with number of hot spots per subject). The number of detected fixation catch trials in baseline and post-training charts – an indirect measure of eye movements – did not correlate significantly with the number of hot spots.

Note that the topographic features analyzed by us were not statistically independent of each other because a significant correlation (Person's Rho) was found on the individual level among all dummy variables of the three feature combinations: 1-2 = 0.85, 1-3 = 0.58, 2-3 = 0.66 (1 = *Residual-Function*, 2 = *Neighbourhood-Residual-Function*, 3 = *Distance-to-Scotoma-Border*).

4. Discussion

The overall goal of the study was to find possible rules in the baseline visual field topography in hemianopic patients that relate to the development of restoration "hot spots" after visual training. This would not only shed light on possible neurobiological mechanisms of perceptual learning after brain damage, but it might open up the possibility to predict the location and extent of restoration in visual fields (Guenther et al., 2009).

We found that visual field areas had a higher probability of becoming vision restoration "hot spots" if they had greater local residual vision (a more shallow defect depth), more residual activity in a spatially limited surround of 5° of visual angle and if they were located closer than 4 mm from the scotoma border in cortical coordinates. Firstly, our findings confirm the special role of residual structures in visual field restoration which is likely mediated by partially surviving neuronal elements. Because the immediate, but not the distant, surround influenced outcome, we propose that lateral interactions, known to play a role in perceptual learning and receptive field plasticity, contribute to vision restoration. This principle of "spatial limitation" of vision restoration is compatible with receptive field studies from other laboratories.

Various animal studies revealed physiological correlates of stimulation-induced recovery of vision after brain lesions. For example, visual stimulation (experience) after retinal or cortical lesion in cats caused a 5-fold receptive field expansion (Pettet and Gilbert,

1992) and neurons close to the cortical lesion border (<1 mm) showed significant receptive field enlargements of 0.4°–0.8° already after 1 hour of visual stimulation (Schweigart and Eysel, 2002). Additionally, the reorganisation of cortical tissue was simulated in a theoretical study, where the perilesion excitability was found to be a critical factor determining reorganisation after cortical stroke in the sensorimotor cortex (Goodall et al., 1997). Similarly, in the computational models of cortical plasticity in the visul system, increased neuronal activity has been shown to be crucial for experimental reorganization of RFs in the peri-lesion zone in MT (Sober et al., 1997) or in the deafferented zone in the V1 following retinal lesion (Young et al., 2007). Taken together, neuronal activity in the affected area seems to be an essential factor required for receptive field plasticity, and these neurophysiological observations guided our interpretation of observed behavioral findings. Although we defined residual function by the ability to detect above-threshold stimuli – which includes both the perception of the stimulus and the execution of the motor response – we assumed that this measure is a simple and useful example of rudimentary visual functions to probe the functionality of the local areas throughout the visual field. Our analyses were based on the assumption that the functional state (full functionality, partial functionality, or complete loss of functionality) represents the degree of structural damage of neural tissue in the visual cortex (intact, partial defect /residual neurons, or full loss), though so far we have only indirect evidence for this from rat studies (Sabel, 1999).

We have first examined whether local *Residual-Function* of each spot in the visual field influenced the extent of restoration, hence whether moderate-defect spots had a higher restoration potential to become hot spots than absolute-defect spots. Indeed, the number of moderate-defect spots was highly correlated with the number of hot spots (Pearson's Rho = 0.7, $p < 0.01$) which supports our hypothesis that local residual activity at baseline (moderate-defects) is an important factor of restoration. We found that the greater the defect depth, the lower the probability of recovery. We have previously hypothesized (Kasten et al., 2000; Sabel et al., 2011a) that areas of residual vision are the preferred location for restoration and that the training forces subjects to focus their attention on "compromised" sectors of the visual field which are partially damaged (Sabel et al., 2011a) which is supported by the observation that focal attention enhances restoration. The training in our subjects involved repetitive activation by massive visual stimulation (about 500.000 stimuli are presentated during the 6 months training course) and such extensive training is typically required to induce perceptual learning (Levi and Polat, 1996).

Besides being influenced by local residual activity, restoration depends also on the activation of the immediate spatial surround. We interpret this lateral influence as a sign of receptive field reorganization that was induced by perceptual learning in the border region of the scotoma. We cannot tell at this time if this reorganization involves a shrinkage or expansion of receptive fields and or their location. Given that cortical reorganization leads to excitability changes in perilesion areas (Goodall et al., 1997) and receptive field plasticity is restricted to the immediate perilesion area (Schweigart and Eysel, 2002), one would expect that an active surround would potentiate restoration potential through lateral influences. Indeed, hot spots had significantly greater baseline residual function (shallower defect depth) in their surround (within a 5° radius) than cold spots. On average, more than one third of all spots within the immediate neighbourhood of hot spots were found to be "healthy" at baseline in comparison to only 1/10 in the surround of cold spots. Accordingly, the number of vision restoration hot spots correlated significantly with greater residual activity in their surround at baseline (Pearson's Rho = 0.56).

Could it be that the difference of residual activity between cold and hot spots is not limited to just 5° but extends far beyond? To address this issue we calculated the residual capacity of the complete hemifield excluding the 5° radius around the spot and found that the residual capacity of hot and cold spots were rather similar. This was confirmed by a separate analysis of a "corridor" of higher spatial resolution. Again, the surround of hot and cold spots differed maximally at directly adjacent locations (<4 mm) and this cold/hot spot difference decreased with distance. Hence, the influence of residual activity around hot spots is spatially limited and restoration is not influenced much by residual activity at greater distances.

Given that residual activity of a local region and its immediate surround correlates significantly with the emergence of restoration hot spots, we now propose that repetitive activation of partially damaged brain regions (here by training) stimulates neuronal reorganization in the deafferented region and its immediate surround. This is in agreement with a study by

Raemaekers et al. (2011) who presented direct evidence for receptive field plasticity: in hemianopic patients participating in vision restoration training, receptive field changes were observed in visual cortex. This finding confirms our conclusion that lateral interactions play a special role in vision restoration. The authors concluded that small visual field enlargements (such as those at the border region of the visual field) can be explained by this "local" receptive field plasticity. But massive visual field expansions seen in some patients cannot be explained by this local interactions mechanism.

The spatial limitation of vision restoration is probably attributed to the architecture of lateral interactions in cortical neuronal network which involve intrinsic horizontal connections in V1 that connect neurons with overlapping receptive fields and neurons with non-overlapping receptive fields of the same preference (Sincich and Blasdel, 2001), such as columns of similar ocular dominance (Malach et al., 1993) or preferred orientation (Gilbert and Wiesel, 1989). Another possible mediator of residual activation are extrastriate connections (Shmuel et al., 2005) which could directly be altered to provide a source for top-down influence via feedback loops to V1. It was hypothesized already that the cortex can reorganize by unmasking of subthreshold activation to supra-threshold levels and this, in turn, could be mediated by horizontal connections in visual cortex (Das and Gilbert, 1995). It was further proposed that these kinds of cortical interconnections play a fundamental role not only in normal visual perception but also in cortical plasticity during perceptual learning in the normal and the damaged brain (Gilbert et al., 2000, 2009; Das and Gilbert, 1995) and they may well contribute to permanent reorganization of neuronal networks (Stettler et al., 2006).

To be able to compare our study results of lateral influences with the values known from the animal literature, we first estimated the size of spatial influences in cortical coordinates using a retinotopic model (considering cortical magnification). We then measured the distances of restored spots to the scotoma border from which the activity of healthy areas might mediate restoration. Hot spots were mostly located in close proximity to the scotoma border: 75% of all hot spots were located at a distance <4 mm from the baseline scotoma border, i.e. a value which is in the range of the lateral influences found in animals (see below). This finding is supported by a significant correlation (Pearson's Rho = 0.44, $p = 0.04$) between the number of impaired spots with close proximity to the scotoma border and the number of hot spots. Note, however, that many hot spots were also located at greater distances (>20 mm) away; so some hot spots clearly exceed by far this distance limitation from the scotoma border (<4 mm). We believe that this is not at variance with the idea of local influences but the restoration probably results from activation of "islands" of residual vision deep inside the blind field which is known to possess much residual potential described by others (Wüst et al., 2002) and which can be improved by training as well (Sahraie et al., 2006, Jobke et al., 2009).

The lateral influences found by us (cortical distance of up to 4 mm or 5 degrees of visual angle) roughly correspond to animals values showing spatially limited propagation of activity. Minimum response fields in V1 of macaques are in the range of 0.5°–3° parafoveal and 1°–9° in peripheral eccentricities <12° (Levitt and Lund, 2002) and V1 intrinsic connections are in a range of 7 mm at 0.75 mm periodicity (Stettler et al., 2002). Feedback projections from V2 which interconnect neurons in V1 were found in the range of 2.82 mm in the owl monkey (Shmuel et al., 2005) and in the range of 7 mm in the macaque at 0.5 mm periodicity (Stettler et al., 2002). So the values observed in animal experiments by others are roughly in the range of lateral influences we have seen in our patients.

In contrast, the average distance of cold spots to the scotoma border was two times greater compared to hot spots. This is obviously in part a result of the fact that the actual deficit – especially in cases of complete hemianopia – extends far into the periphery.

Our results of the topographic influences should be interpreted with caution because the scotoma border and the respective residual state of individual regions are only defined functionally, i.e., by a behavioral perimetry task. So far we were not able to directly visualise these areas anatomically in the cortex but this would clearly be of interest in future studies and imaging studies would be helpful to accomplish this goal.

To determine if eye movement artifacts can explain our findings, we have estimated their influence by measuring fixation quality in all subjects using a colour-based fixation catch trial paradigm which is most sensitive to eye movements >2° (unpublished observations). If vision restoration is an eye movement artifact, one would have expected that patients with poor fixation performance had more hot spots, which is not what was found. Furthermore, eye tracker record-

ing found that 95% and 99% of all eye movements during HRP are within 2° at baseline or at post-training diagnostic sessions, respectively (Kasten et al., 2006). Also, if eye movements explained the restoration, the hot spots would have occurred anywhere in the visual field and this was also not the case. Thus, there is no evidence that eye movements can explain our findings (for discussion, see Sabel et al., 2011a, b).

In summary, vision restoration is significantly associated with topographic features of the baseline visual field charts. If a visually tested position (spot) has a poor detection performance at baseline (absolute or severe-defect), its restoration potential is smaller than if it has a greater amount of residual vision (mild or moderate defect depth). The same rule holds for the immediate spatial neighbourhood, i.e. hot spots are significantly associated with greater baseline residual vision in their immediate surround than cold spots. Interestingly, the spatial extent of such neighbourhood influences was maximal only in the directly adjacent spatial surround and was reduced with increasing neighbourhood radius. This suggests that neuronal structures mediating local restoration of vision are limited in spatial extent as the majority (75%) of all hot spots are located close to the scotoma border (i.e., <4 mm away).

Our observations are compatible with the hypothesis that activation of residual vision mediates vision restoration after visual system damage (Sabel et al., 2011b) and that there is a special role of cortical propagators of activation through lateral interactions (like lateral influences in V1 and feedback connections from V2). While the local nature of the lateral interaction might provide a structural limit of local vision restoration, some clinical cases with significant vision restoration deep in the field cannot be explained by such lateral influences. Here, other more global mechanisms of vision restoration should be explored, especially those involving extrastriate, retinofugal pathways unaffected by the cortical damage (Sahraie et al., 2006) or larger neuronal networks throughout the brain.

Acknowledgements

The study was supported by "BMBF: InnoRegio-InnoMed, funding number 03I0415D" and the BMBF Project ERA-net Neuron "REVIS" (01EW1210) to B. Sabel; F. Wolf was supported by BMBF (funding numbers 01GQ1005B, 01GQ0811, 01GQ0922) and the DFG (SFB 889).We thank Dr. S. Kropf for his statistics advice and Dr. Torsten Wiesel for an in-depth discussion of the findings and their interpretation.

References

Andrews, T.J., Halpern, S.D., & Purves, D. (1997). Correlated size variations in human visual cortex, lateral geniculate nucleus, and optic tract. *J Neurosci*, *17*, 2859-2868.

Balasubramanian, M., Polimeni, J., & Schwartz, E.L. (2002). The V1-V2-V3 complex: Qasiconformal dipole maps in primate striate and extra-striate cortex. *Neural Netw*, *15*, 1157-1163.

Bergsma, D.P., & Van der Wildt, G.J. (2008). Properties of the regained visual field after visual detection training of hemianopia patients. *Restor Neurol Neurosci*, *26*, 365-375.

Buonomano, D.V., & Merzenich, M.M. (1998). Cortical plasticity: From synapses to maps. *Annu Rev Neurosci*, *21*, 149-186.

Calford, M.B., Wang, C., Taglianetti, V., Waleszczyk, W.J., Burke, W., & Dreher, B. (2000). Plasticity in adult cat visual cortex (area 17) following circumscribed monocular lesions of all retinal layers. *J Physiol*, *524*, 587-602.

Calford, M.B., Wright, L.L., Metha, A.B., & Taglianetti, V. (2003). Topographic plasticity in primary visual cortex is mediated by local corticocortical connections. *J Neurosci*, *23*, 6434-6442.

Das, A., & Gilbert, C.D. (1995). Long- range horizontal connections and their role in cortical reorganisation revealed by optical recording of cat primary visual cortex. *Nature*, *375*, 780-784.

Dougherty, R.F., Koch, V.M., Brewer, A.A., Fischer, B., Modersitzki, J., & Wandell, B.A. (2003). Visual field representations and locations of visual areas V1/2/3 in human visual cortex. *J Vis*, *3*, 586-598.

Fedorov, A.B., Jobke, S., Bersnev, V., Chibisova, A., Chibisova, Y., Gall, C., & Sabel, B.A. (2011). Restoration of vision after optic nerve lesions with non-invasive transorbital alternating current stimulation: A clinical observational study. *Brain Stimul*, *4*, 189-201.

Gall, C., Fedorov, A.B., Ernst, L., Borrmann, A., & Sabel, B.A. (2010). Repetitive transorbital alternating current stimulation (rtACS) in optic neuropathy – single case study. *NeuroRehabilitation*, *27*(4), 335-341.

Gall, C., Sgorzaly, S., Schmidt, S., Brandt, S., Fedorov, A., & Sabel, B.A. (2011). Noninvasive transorbital alternating current stimulation improves subjective visual functioning and vision-related quality of life in optic neuropathy. *Brain Stimul*, *4*, 175-188.

Giannikopoulos, D.V., & Eysel, U.T. (2006). Dynamics and specificity of cortical map reorganisation after retinal lesions. *Proc Natl Acad Sci U S A*, *103*, 10805-10810.

Gilbert, C., Ito, M., Kapadia, M., & Westheimer, G. (2000). Interactions between attention, context and learning in primary visual cortex. *Vision Res*, *40*, 1217-1226.

Gilbert, C.D. (1994). Neuronal dynamics and perceptual learning. *Curr Biol*, *4*, 627-629.

Gilbert, C.D., Li, W., & Piech, V. (2009). Perceptual learning and adult cortical plasticity. *J Physiol*, *587*, 2743-2751.

Gilbert, C.D., & Wiesel, T.N. (1989). Columnar specificity of intrinsic horizontal and corticocortical connections in cat visual cortex. *J Neurosci*, *9*, 2432-2442.

Gilbert, C.D., & Wiesel, T.N. (1992). Receptive field dynamics in adult primary visual cortex. *Nature*, *356*, 150-152.

Goodall, S., Reggia, J.A., Chen, Y., Ruppin, E., & Whitney, C. (1997). A computational model of acute focal cortical lesions. *Stroke*, *28*, 101-109.

Gudlin, J., Mueller, I., Thanos, S., & Sabel, B.A. (2008). Computer based vision restoration training in glaucoma patients – a small open pilot study. *Restor Neurol Neurosci*, *26*, 403-412.

Guenther, T., Mueller, I., Preuss, M., Kruse, R., & Sabel, B.A. (2009). Treatment outcome prediction model of visual field recovery using Self-Organizing-Maps. *IEEE Trans Biomed Eng*, *56*(3), 572-581.

Heinen, S.J., & Skavenski, A.A. (1991). Recovery of visual responses in foveal V1 neurons following bilateral foveal lesions in adult monkey. *Exp Brain Res*, *83*, 670-674.

Henriksson, L., Raninen, A., Nasanen, R., Hyvarinen, L., & Vanni, S. (2007). Training-induced cortical representation of a hemianopic hemifield. *J Neurol Neurosurg Psychiatry*, *78*, 74-81.

Jobke, S., Kasten, E., & Sabel, B.A. (2009). Vision restoration through extrastriate stimulation in patients with visual field defects -a double-blind and randomized experimental study. *Neurorehabil Neural Repair*, *23*(3), 246-255.

Julkunen, L., Tenovuo, O., Jaaskelainen, S., & Hamalainen, H. (2003). Rehabilitation of chronic post-stroke visual field defect with computer-assisted training: A clinical and neurophysiological study. *Restor Neurol Neurosci*, *21*, 19-28.

Julkunen, L., Tenovuo, O., Vorobyev, V., Hiltunen, J., Teras, M., Jääskeläinen, S.K., & Hämäläinen, H. (2006). Functional brain imaging, clinical and neurophysiological outcome of visual rehabilitation in a chronic stroke patient. *Restor Neurol Neurosci*, *24*, 123-132.

Kasten, E., Bunzenthal, U., & Sabel, B.A. (2006). Visual field recovery after vision restoration therapy (VRT) is independent of eye movements: An eye tracker study. *Behav Brain Res*, *175*, 18-26.

Kasten, E., Poggel, D.A., Müller-Oehring, E., Gothe, J., Schulte, T., & Sabel, B.A. (1999). Restoration of vision II: Residual functions and training-induced visual field enlargement in brain-damaged patients. *Restor Neurol Neurosci*, *15*, 273-287.

Kasten, E., Poggel, D.A., & Sabel, B.A. (2000). Computer-based training of stimulus detection improves colour and simple pattern recognition in the defective field of hemianopic subjects. *J Cogn Neurosci*, *12*, 1001-1012.

Kasten, E., Strasburger, H., & Sabel, B.A. (1997). Programs for diagnosis and therapy of visual field deficits in vision rehabilitation. *Spat Vis*, *10*, 499-503.

Kasten, E., Wust, S., Behrens-Baumann, W., & Sabel, B.A. (1998). Computer-based training for the treatment of partial blindness. *Nat Med*, *4*, 1083-1087.

Levi, D.M., & Polat, U. (1996). Neural plasticity in adults with amblyopia. *Proc Natl Acad Sci U S A*, *93*(13), 6830-6834.

Levitt, J.B., & Lund, J.S. (2002). The spatial extent over which neurons in macaque striate cortex pool visual signals. *Vis Neurosci*, *19*, 439-452.

Malach, R., Amir, Y., Harel, M., & Grinvald, A. (1993). Relationship between intrinsic connections and functional architecture revealed by optical imaging and *in vivo* targeted biocytin injections in primate striate cortex. *Proc Natl Acad Sci U S A*, *90*, 10469-10473.

Marshall, R.S., Ferrera, J.J., Barnes, A., Xian, Z., O'Brien, K.A., Chmayssani, M., Hirsch, J., & Lazar, R.M. (2008). Brain activity associated with stimulation therapy of the visual borderzone in hemianopic stroke patients. *Neurorehabil Neural Repair*, *22*(2), 136-144.

Mueller, I., Poggel, D.A., Kenkel, S., Kasten, E., & Sabel, B.A. (2003). Vision restoration therapy after brain damage: Subjective improvements of activities of daily life and their relationship to visual field enlargements. *Visual Impairment Research*, *5*, 157-178.

Pettet, M.W., & Gilbert, C.D. (1992). Dynamic changes in receptive-field size in cat primary visual cortex. *Proc Natl Acad Sci U S A*, *89*, 8366-8370.

Pleger, B., Foerster, A.F., Widdig, W., Henschel, M., Nicolas, V., Jansen, A., Frank, A., Knecht, S., Schwenkreis, P., & Tegenthoff, M. (2003). Functional magnetic resonance imaging mirrors recovery of visual perception after repetitive tachistoscopic stimulation in patients with partial cortical blindness. *Neurosci Lett*, *335*, 192-196.

Poggel, D.A., Kasten, E., & Sabel, B.A. (2004). Attentional cueing improves vision restoration therapy in patients with visual field defects. *Neurology*, *63*, 2069-2076.

Polat, U. (2008). Restoration of underdeveloped cortical functions: Evidence from treatment of adult amblyopia. *Restor Neurol Neurosci*, *26*, 413-424.

Raemaekers, M., Bergsma, D.P., van Wezel, R.J., van der, Wildt, G.J., & van den Berg, A.V. (2011). Effects of vision restoration training on early visual cortex in patients with cerebral blindness investigated with functional magnetic resonance imaging. *J Neurophysiol*, *105*, 872-882.

Sabel, B.A. (1999). Restoration of vision I: Neurobiological mechanisms of restoration and plasticity after brain damage - a review. *Restor Neurol Neurosci*, *15*, 177-200.

Sabel, B., Kenkel, S., & Kasten, E. (2004). Vision restoration therapy (VRT) efficacy as assessed by comparative perimetric analysis and subjective questionnaires. *Restor Neurol Neurosci*, *22*, 399-420.

Sabel, B.A., Fedorov, A.B., Naue, N., Borrmann, A., Herrmann, C., & Gall, C. (2011a). Non-invasive alternating current stimulation improves vision in optic neuropathy. *Restor Neurol Neurosci*, *29*, 493-505.

Sabel, B.A., Henrich-Noack, P., Fedorov, A., & Gall, C. (2011 b).Vision restoration after brain damage: The "Residual Vision Activation Theory". *Prog Brain Res*, *192*, 199-262.

Sabel, B.A., & Kasten, E. (2000). Restoration of vision by training of residual functions. *Curr Opin Ophthalmol*, *11*, 430-436.

Sahraie, A., Trevethan, C.T., MacLeod, M.J., Murray, A.D., Olson, J.A., & Weiskrantz, L. (2006). Increased sensitivity after repeated stimulation of residual spatial channels in blindsight. *Proc Natl Acad Sci U S A*, *103*(40), 14971-14976.

Schwartz, E.L. (1977). Spatial mapping in the primate sensory projection: Analytic structure and relevance to perception. *Biol Cybern*, *25*, 181-194.

Schweigart, G., & Eysel, U.T. (2002). Activity-dependent receptive field changes in the surround of adult cat visual cortex lesions. *Eur J Neurosci*, *15*, 1585-1596.

Shmuel, A., Korman, M., Sterkin, A., Harel, M., Ullman, S., Malach, R., & Grinvald, A. (2005). Retinotopic axis specificity and selective clustering of feedback projections from V2 to V1 in the owl monkey. *J Neurosci*, *25*, 2117-2131.

Sincich, L.C., & Blasdel, G.G. (2001). Oriented axon projections in primary visual cortex of the monkey. *J Neurosci*, *21*, 4416-4426.

Sober, S.J., Stark, J.M., Yamasaki, D.S., & Lytton, W.W. (1997). Receptive field changes after strokelike cortical ablation: A role for activation dynamics. *J Neurophysiol*, *78*, 1-6.

Stettler, D.D., Das, A., Bennett, J., & Gilbert, C.D. (2002). Lateral connectivity and contextual interactions in macaque primary visual cortex. *Neuron*, *36*, 739-750.

Stettler, D.D., Yamahachi, H., Li, W., Denk, W., & Gilbert, C.D. (2006). Axons and synaptic boutons are highly dynamic in adult visual cortex. *Neuron*, *49*, 877-887.

Waleszczyk, W.J., Wang, C., Young, J.M., Burke, W., Calford, M.B., & Dreher, B. (2003). Laminar differences in plasticity in area 17 following retinal lesions in kittens or adult cats. *Eur J Neurosci*, *17*, 2351-2368.

Watanabe, T., Nanez, J.E. Sr., Koyama, S., Mukai, I., Liederman, J., & Sasaki, Y. (2002). Greater plasticity in lower-level than higher-level visual motion processing in a passive perceptual learning task. *Nat Neurosci*, *5*, 1003-1009.

Wüst, S., Kasten, E., & Sabel, B.A. (2002). Blindsight after optic nerve injury indicates functionality of spared fibers. *J Cogn Neurosci*, *14*, 243-253.

Young, J.M., Waleszczyk, W.J., Wang, C., Calford, M.B., Dreher, B., & Obermayer, K. (2007). Cortical reorganization consistent with spike timing-but not correlation-dependent plasticity. *Nat Neurosci*, *10*, 887-895.

Zhang, X., Kedar, S., Lynn, M.J., Newman, N.J., & Biousse, V. (2006). Natural history of homonymous hemianopia. *Neurology*, *66*, 901-905.

Zihl, J., & Cramon, D. (1985). Visual field recovery from scotoma in patients with postgeniculate damage. A review of 55 cases. *Brain*, *108*, 335-365.